Hindawi Publishing Corporation
EURASIP Journal on Wireless Communications and Networking
Volume 2007, Article ID 89780, 9 pages
doi:10.1155/2007/89780

Research Article

On Sum Rate and Power Consumption of Multi-User Distributed Antenna System with Circular Antenna Layout

Jiansong Gan, Yunzhou Li, Limin Xiao, Shidong Zhou, and Jing Wang

Department of Electronic Engineering, Tsinghua University, Room 4-405 FIT Building, Beijing 100084, China

Received 18 November 2006; Accepted 29 July 2007

Recommended by Petar Djuric

We investigate the uplink of a power-controlled multi-user distributed antenna system (DAS) with antennas deployed on a circle. Applying results from random matrix theory, we prove that for such a DAS, the per-user sum rate and the total transmit power both converge as user number and antenna number go to infinity with a constant ratio. The relationship between the asymptotic per-user sum rate and the asymptotic total transmit power is revealed for all possible values of the radius of the circle on which antennas are placed. We then use this rate-power relationship to find the optimal radius. With this optimal radius, the circular layout DAS (CL-DAS) is proved to offer a significant gain compared with a traditional colocated antenna system (CAS). Simulation results are provided, which demonstrate the validity of our analysis.

1. INTRODUCTION

Information theory suggests that for a system with a large number of users, increasing the number of antennas at the base station leads to a linear increase in sum-rate capacity without additional power or bandwidth consumption [1]. However, previous studies have mostly focused on scenarios with all antennas colocated at the base station. Suppose antennas are connected but placed with geographical separations, each user will be more likely to be close to some antennas, and the transmit power can therefore be saved. This is the concept of distributed antenna system (DAS) which was originally introduced for coverage improvement in indoor wireless communications [2].

Recent interests in DAS have shifted to advantages in capacity or sum rate. The channel capacity of a single-user DAS and the sum rate of a multi-user DAS were investigated and compared with those of co-located antenna systems (CAS) using Monte Carlo simulation in [3] and [4], respectively, where significant improvements have been observed. However, these works did not provide theoretical analysis to characterize the exact gain that a DAS offers over a CAS. Neither did they present optimal parameters for antenna deployment.

Another line of work introduces coordination between base stations and suggests an architecture quite similar to DAS [5]. Sum rate of such a system has been studied in [6, 7]. However, unlike investigations in DAS which evaluate performance improvement by scattering co-located antennas, these works mainly assess performance enhancement by introducing coordination between base stations. In addition, analysis in [7], for example, assumes a large number of antennas co-located at the base station, which differs from ideas of DAS.

In this study, we demonstrate the advantage of scattering co-located antennas in an analytical way. Though there are different ways to scatter antennas and different antenna layouts may result in different performances, investigating all possible layouts is rather difficult. For analytical tractability we only consider a special DAS with antennas deployed on a circle. A similar model has been used in [8] to study the capacity of CDMA system with distributed antennas. Since distributed antennas are relatively cheap, it is feasible to deploy a large number of antennas, which makes application of random matrix theory possible. Applying recent results from this theory, we prove that for a circular-layout DAS (CL-DAS), the per-user sum rate and the total transmit power both converge as user number and antenna number go to infinity with a constant ratio. Then, the relationship between the asymptotic per-user sum rate and the asymptotic total transmit power is disclosed for all possible values of the radius of the circle on which antennas are deployed. We further show how the rate-power relationship can be used to find the optimal radius. A CL-DAS with this optimal radius

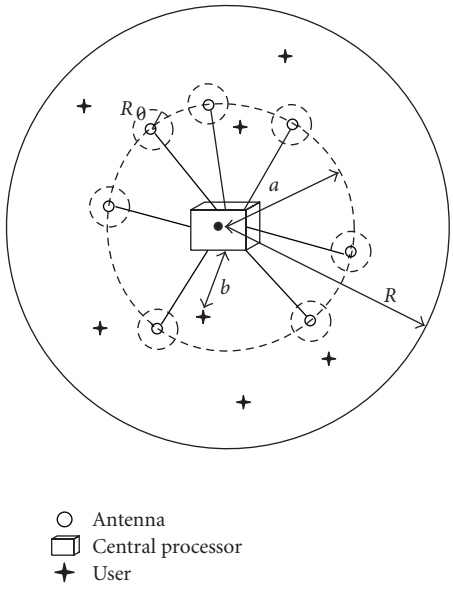

Figure 1: Illustration of CL-DAS.

is proved to offer a significant gain over a traditional CAS. Though the maximum achievable gain that a general layout DAS provides over a CAS has not been found yet, it can be lower bounded by the presented gain for the optimized CL-DAS (OCL-DAS). Hence, we demonstrate the possibility of great performance enhancement by scattering the centralized antennas.

The remainder of this paper is organized as follows. Section 2 describes the system model. Sum rate, power consumption, and their relationship are analyzed in Section 3. In Section 4, we show how to use the rate-power relationship for antenna deployment optimization and how much gain can be obtained. Simulation results can be found in Section 5. Finally, concluding remarks are given in Section 6.

2. SYSTEM MODEL

Before proceeding further, we first explain the notations used in this paper. All vectors and matrices are in boldface, $\mathbf{X}^T$ and $\mathbf{X}^H$ are the transpose and the conjugate transpose of $\mathbf{X}$, respectively, $\mathbf{X}_{i,j}$ is the (i, j)th element of $\mathbf{X}$, $\mathbf{X}_{i,:}$ is the ith row of $\mathbf{X}$, $\mathbf{X}_{:,j}$ is the jth column of $\mathbf{X}$, and $\mathcal{E}$ is the expectation operator.

As illustrated in Figure 1, an isolated coverage area of radius R is considered. To describe antenna and user distributions, we use polar coordinates (r, θ) relative to the center of the coverage area. The CL-DAS under study consists of N antennas which are independent and uniformly distributed on the circle with $r = a$. (We do not assume deterministic deployment scheme here, considering that the complex terrain may make deploying a large number of antennas with determinate positions difficult.) These antennas are connected to the central processor via optical fibers. K single-antenna users are mutually independent and uniformly distributed in the coverage area excluding the radius R_0 neighborhood of each antenna [9]. To describe user distribution, b is used to denote user polar radius in the following analysis.

2.1. Signal model

Let x_k and p_k be the transmitted signal with unit energy and the transmit power of the kth user, respectively. Let $\mathbf{h}_k \in \mathbb{C}^{N\times 1}$ denote the vector channel between the kth user and the distributed antennas. Then, the received signal $\mathbf{y} \in \mathbb{C}^{N\times 1}$ can be expressed as

$$\mathbf{y} = \sum_{k=1}^{K} \mathbf{h}_k \sqrt{p_k} x_k + \mathbf{n} = \mathbf{H}\mathbf{P}^{1/2}\mathbf{x} + \mathbf{n}, \tag{1}$$

where $\mathbf{x} = [x_1, x_2, \ldots, x_K]^T$ is the transmitted signal vector, $\mathbf{P} = \mathrm{diag}(p_1, p_2, \ldots, p_K)$ is the transmit power matrix, $\mathbf{n} \in \mathbb{C}^{N\times 1}$ is the noise vector with distribution $\mathcal{CN}(0, \sigma_n^2 \mathbf{I}_N)$, and $\mathbf{H} = [\mathbf{h}_1, \mathbf{h}_2, \ldots, \mathbf{h}_K]$ is the channel matrix. Since antennas are geographically separated, to model DAS channel, we should encompass not only small-scale fading but also large-scale fading. Here, we model $\mathbf{H}$ as

$$\mathbf{H} = \mathbf{L} \circ \mathbf{H}_w, \tag{2}$$

where "$\circ$" is the Hadamard product or element-wise product, $\mathbf{H}_w$, a matrix with independent and identically distributed (i.i.d.), zero mean, unit variance, circularly symmetric complex Gaussian entries, reflects the small-scale fading, and $\mathbf{L}$ represents large-scale fading between users and antennas. Adding shadowing to path loss model used in [3], we model entries of $\mathbf{L}$ as

$$\mathbf{L}_{n,k} = \sqrt{D_{n,k}^{-\gamma} S_{n,k}}, \quad R_0 \le D_{n,k} < 2R \ \forall n, k, \tag{3}$$

where $D_{n,k}$ and $S_{n,k}$ are independent random variables representing the distance and the shadowing between the nth antenna and the kth user, respectively, γ is the path loss exponent. $\{S_{n,k} \mid n = 1, 2, \ldots, N,\ k = 1, 2, \ldots, K\}$ are i.i.d. random variables with probability density function (pdf),

$$f_S(s) = \frac{1}{\sqrt{2\pi}\lambda\sigma_s s} \exp\left(-\frac{(\ln s)^2}{2\lambda^2\sigma_s^2} \right), \quad s > 0, \tag{4}$$

where σ_s is the shadowing standard derivation in dB and $\lambda = \ln 10/10$. Since these $S_{n,k}$s are i.i.d., we will not distinguish them in the following analysis and simply use S instead.

We note that the system model used in this study differs from that in [6, 7] where the large-scale fading part $\mathbf{L}$ is assumed to be fixed. A fixed $\mathbf{L}$ is applicable for performance comparison between systems with and without coordination, since coordination does not impact $\mathbf{L}$. However, this fixed $\mathbf{L}$ does not apply to performance comparison between CAS and DAS, since it cannot fully reflect the large-scale fading between antennas and users for different antenna layouts. Therefore, a stochastic $\mathbf{L}$ must be included, which makes our work quite different from analyses in [6, 7].

Power allocation policy impacts system performance to a great extent. To investigate performance of DAS, we assume a power control scheme widely used in CDMA systems, with

which all users are guaranteed to arrive at the same power level. The power control scheme is given by

$$p_k \sum_{n=1}^{N} \mathbf{L}_{n,k}^2 = P_R \quad \forall k, \tag{5}$$

where P_R is the required receiving power level.

2.2. Distance distributions

As distances between users and antennas impact the channel directly, a key problem for the performance analysis is to investigate their characteristics. Since they are random variables, we characterize them by presenting their distribution functions.

Although radius of the circle for antenna deployment can be optimized, it is a constant once chosen. So in the following analysis, we first consider an arbitrary a and establish a rate-power relationship between the asymptotic per-user sum rate and the asymptotic total transmit power. Then, we optimize a to get the best performance. As antennas are mutually independent and uniformly distributed on the circle, their polar angles $\Theta_{a1}, \Theta_{a2}, \ldots, \Theta_{aN}$ are i.i.d. random variables with pdf,

$$f_{\Theta_a}(\theta_a) = \frac{1}{2\pi}, \quad 0 \le \theta_a < 2\pi. \tag{6}$$

Since users cannot fall into the radius R_0 neighborhood of each antenna, when there are a large number of antennas, users cannot fall into the area such that the polar radius b satisfies $|b - a| < R_0$. As users are mutually independent and uniformly distributed, the polar radiuses of the K users $B_1, B_2, \ldots, B_K$ are i.i.d. random variables with pdf,

$$f_B(b) = \frac{b}{\int_{r\in\mathcal{B}} r\,\mathrm{d}r}, \quad b \in \mathcal{B}, \tag{7}$$

where $\mathcal{B} = \{b \mid 0 \le b \le R, |b-a| \ge R_0\}$ is the effective coverage area. The polar angles of the K users $\Theta_{u1}, \Theta_{u2}, \ldots, \Theta_{uK}$ are i.i.d. random variables with pdf

$$f_{\Theta_u}(\theta_u) = \frac{1}{2\pi}, \quad 0 \le \theta_u < 2\pi. \tag{8}$$

We characterize the distance distributions from two aspects: the perspective of a user and the perspective of an antenna. Consider a user indexed k, we assume its polar radius is b and polar angle is θ_u. Then, the distance between this user and the nth antenna can be expressed as

$$D_{n,k} = \sqrt{a^2 + b^2 - 2ab\cos\left(\Theta_{an} - \theta_u\right)} \quad \forall n. \tag{9}$$

Since $\Theta_{a1}, \Theta_{a2}, \ldots, \Theta_{aN}$ are i.i.d. random variables with pdf (6), distances from this user to all antennas $D_{1,k}$, $D_{2,k}, \ldots, D_{N,k}$ are i.i.d. random variables with cumulative distribution function (cdf):

$$F_{D|B}(d \mid b) = Pr(D \le d \mid B = b) = \begin{cases} 0 & \text{if } d < |a-b|, \\ 1 & \text{if } d \ge a+b, \\ \dfrac{1}{\pi}\arccos\left(\dfrac{a^2+b^2-d^2}{2ab}\right), & \text{otherwise.} \end{cases} \tag{10}$$

Since antennas are symmetric, distance distributions for all antennas are the same. Without loss of generality, we consider an antenna indexed n. When the polar radius of the kth user is b, distribution of $D_{n,k}$ is the same as (10). Averaging the distribution over all possible user polar radius, we get the cdf of $D_{n,k}$,

$$F_D(d) = \int_{b\in\mathcal{B}} F_{D|B}(d \mid b) f_B(b)\mathrm{d}b. \tag{11}$$

Since users are mutually independent and uniformly distributed, distances from the nth antenna to all users $D_{n,1}, D_{n,2}, \ldots, D_{n,K}$ are i.i.d. random variables with cdf (11).

3. ASYMPTOTIC ANALYSIS

When instantaneous channel state information is available at the receiver side but not at the transmitter side, the sum rate, normalized by the number of users, can be expressed as [10]

$$C = \frac{1}{K}\log_2 \det\left(\mathbf{I}_N + \frac{1}{\sigma_n^2}\mathbf{HPH}^H\right). \tag{12}$$

Unfortunately, (12) depends on distances, shadowing, and small-scale fading between antennas and users which are random variables. Hence, it is random and difficult to evaluate.

To assess the cost of the system, we introduce a metric called total transmit power which can be defined as

$$E \triangleq \sum_{k=1}^{K} p_k = \sum_{k=1}^{K} \frac{P_R}{\sum_{n=1}^{N} \mathbf{L}_{n,k}^2}, \tag{13}$$

where the second equality follows from (5). Equation (13) is also a random variable depends on distances and shadowing between antennas and users.

In this section, we prove as $N, K \to \infty$ with $K/N \to \beta$, both the per-user sum rate and the total transmit power converge to their respective asymptotic values. To prove this convergence, we first cite some definitions and results from random matrix theory.

3.1. Definitions and preliminary results

Definition 1. Given a vector $\mathbf{v} = [v_1, v_2, \ldots, v_N]$, its empirical distribution function (edf) is defined as

$$F_N(x) \triangleq \frac{1}{N}\sum_{n=1}^{N} I_{[v_n,\infty)}(x), \tag{14}$$

where $I_A(w)$ is the indicator function taking value 1 if $w \in A$ and 0 otherwise. If $F_N(\cdot)$ converges as $N \to \infty$, its limit (the asymptotic edf) is denoted by $F(\cdot)$.

The following proposition is a reformulation of some theorems presented in [11, 12], which provides a theoretical support for our analysis.

Proposition 1. *Consider an $N \times K$ matrix $\mathbf{H} = \mathbf{L} \circ \mathbf{H}_w$ with $\mathbf{L}$ and $\mathbf{H}_w$ independent $N \times K$ random matrices. Entries of $\mathbf{H}_w$ are independent, zero mean, unit variance, circularly symmetric complex Gaussian variables. Let $\mathbf{G} = \mathbf{L} \circ \mathbf{L}$ be the power gain matrix of $\mathbf{H}$. If for all k, edf of $(\mathbf{G}_{:,k})^T$ converges as $N \to \infty$ to the cdf of a random variable with expectation 1 and all moments bounded, and for all n, edf of $\mathbf{G}_{n,:}$ converges as $K \to \infty$ to the cdf of a random variable with expectation 1 and all moments bounded, the sum rate normalized by the number of transmit antennas converges almost surely as $N, K \to \infty$ with $K/N \to \beta$:*

$$\begin{aligned}\frac{1}{K}\log_2 \det\left(\mathbf{I}_N + \frac{\rho}{K}\mathbf{H}\mathbf{H}^H\right) &\xrightarrow{a.s.} \mathcal{C}(\beta,\rho)\\ &= \log_2\left(1+\frac{\rho}{\beta}-\frac{1}{4}\mathcal{F}\left(\frac{\rho}{\beta},\beta\right)\right)-\frac{\log_2 e}{4\rho}\mathcal{F}\left(\frac{\rho}{\beta},\beta\right)\\ &\quad+\frac{1}{\beta}\log_2\left(1+\rho-\frac{1}{4}\mathcal{F}\left(\frac{\rho}{\beta},\beta\right)\right),\end{aligned} \tag{15}$$

where ρ is the signal-to-noise ratio (SNR) and $\mathcal{F}(\cdot,\cdot)$ is defined as

$$\mathcal{F}(x,z) \triangleq \left(\sqrt{x(1+\sqrt{z})^2+1}-\sqrt{x(1-\sqrt{z})^2+1}\right)^2. \tag{16}$$

3.2. Proof of the convergence and derivation of the rate-power relationship

We have shown that though antenna placement and user distribution are performed in a random manner, distributions of distances between antennas and users are known. With such information, we investigate the distributions of entries of channel matrix $\mathbf{H}$. Since its small-scale fading part $\mathbf{H}_w$ is well modeled as with independent, zero mean, unit variance, circularly symmetric complex Gaussian entries, the rest is to investigate its large-scale fading part. Denote the power gain matrix of $\mathbf{H}$ by $\mathbf{G}$ with $\mathbf{G}_{n,k} = \mathbf{L}_{n,k}^2 = D_{n,k}^{-\gamma} S$, we characterize the distributions of elements of $\mathbf{G}$ from two perspectives: a user's perspective and an antenna's perspective. From (4) and (10), we learn that for a user indexed k, $\mathbf{G}_{1,k}, \mathbf{G}_{2,k}, \ldots, \mathbf{G}_{N,k}$ are i.i.d. random variables with cdf:

$$F_{G|B}(g \mid b) = \int_0^\infty \left(1 - F_{D|B}\left(\left(\frac{g}{u}\right)^{-1/\gamma} \,\middle|\, b\right)\right) f_S(u)\mathrm{d}u, \tag{17}$$

given $B_k = b$. Then, the arithmetical average $1/N \sum_{n=1}^N \mathbf{G}_{n,k}$ can be writen as

$$\mathcal{G}(a,b) \triangleq \mathcal{E}[G \mid B = b] = \exp\left(\frac{1}{2}\lambda^2\sigma_s^2\right) \cdot \mathcal{E}[D^{-\gamma} \mid B = b] \tag{18}$$

$$= \exp\left(\frac{1}{2}\lambda^2\sigma_s^2\right)\frac{1}{\pi}\int_0^\pi \left(a^2+b^2-2ab\cos\theta\right)^{-\gamma/2}\mathrm{d}\theta, \tag{19}$$

according to (4) and (10).

From the perspective of an antenna indexed n, $\mathbf{G}_{n,1}$, $\mathbf{G}_{n,2}, \ldots, \mathbf{G}_{n,K}$ are i.i.d. random variables with cdf

$$F_G(g) = \int_0^\infty \left(1 - F_D\left(\left(\frac{g}{u}\right)^{-1/\gamma}\right)\right) f_S(u)\mathrm{d}u, \tag{20}$$

according to (4) and (11).

From (5), we have

$$p_k = \frac{P_R}{\sum_{n=1}^N \mathbf{L}_{n,k}^2} = \frac{P_R}{\sum_{n=1}^N \mathbf{G}_{n,k}} \quad \forall k. \tag{21}$$

To evaluate (12), we rewrite it to (15)'s form and get the power-controlled equivalent channel $\mathbf{H}_\mathbf{E} = \mathbf{H}\sqrt{K}\mathbf{P}^{1/2}$. According to property of $\mathbf{H}_\mathbf{E}$ and Proposition 1, we present the following proposition:

Proposition 2. *The uplink per-user sum rate of a CL-DAS converges almost surely, as $N \to \infty, K \to \infty$ with $K/N \to \beta$, to*

$$\mathcal{C}\left(\beta, \frac{\beta P_R}{\sigma_n^2}\right). \tag{22}$$

Proof. See appendix. □

To characterize power consumption of a CL-DAS, we investigate the asymptotic behavior of E in (13) when there are a large number of antenna and users. By the strong law of large numbers and the distributions of $\mathbf{G}$'s elements, we have

$$\frac{1}{K}\sum_{k=1}^K \frac{K/N}{1/N\sum_{n=1}^N \mathbf{G}_{n,k}} \xrightarrow{\text{a.s.}} \beta \int_{b\in\mathcal{B}} \frac{1}{\mathcal{G}(a,b)} f_B(b)\mathrm{d}b, \tag{23}$$

as $N, K \to \infty, K/N \to \beta$, where $\mathcal{G}(a,b)$ is defined in (18).

Let

$$\mathcal{P}(a) \triangleq \int_{b\in\mathcal{B}} \frac{1}{\mathcal{G}(a,b)} f_B(b)\mathrm{d}b, \tag{24}$$

we have

$$E \xrightarrow{\text{a.s.}} \beta P_R \mathcal{P}(a). \tag{25}$$

The total transmit power represents the cost of a system, and the per-user sum rate stands for the output. To compare cost-output relationships for different antenna configurations, we establish the relationship between the asymptotic per-user sum rate and the asymptotic total transmit power according to (22) and (25):

$$C = \mathcal{C}\left(\beta, \frac{E}{\mathcal{P}(a)\sigma_n^2}\right). \tag{26}$$

4. DEPLOYMENT OPTIMIZATION AND PERFORMANCE ENHANCEMENT

We learn from (26) that different a results in different rate-power relationship. In CAS, a is fixed to be 0, while it may vary from 0 to R for CL-DAS. Therefore, choosing the optimal radius and achieving the best rate-power relationship is possible. In this section, we will show how to decide the optimal radius and how much gain an optimized CL-DAS offers compared with a CAS.

As $\mathcal{C}(\beta,\rho)$ is a monotonic increasing function of ρ, the optimal radius that minimizes the power consumption for a given sum-rate requirement is the a that minimizes (24). In the same way, this a also leads to the maximum sum rate for a given total transmit power. So the a that minimizes (24) is optimal for antenna deployment in the sense of both power consumption and sum rate.

To evaluate performance enhancement that an OCL-DAS provides over a CAS, we define two metrics. The first is the power gain under the same sum rate constraint, defined as

$$G_p \triangleq 10\log\left(\frac{E_{\text{CAS}}}{E_{\text{OCL-DAS}}}\right), \tag{27}$$

with $C_{\text{OCL-DAS}} = C_{\text{CAS}}$. The second is the per-user sum-rate gain in the high SNR regime under the same total transmit power constraint, defined as

$$G_{c\infty} \triangleq C_{\text{OCL-DAS}} - C_{\text{CAS}} \tag{28}$$

with $E_{\text{OCL-DAS}} \to \infty$, $E_{\text{CAS}} \to \infty$, and $E_{\text{OCL-DAS}} = E_{\text{CAS}}$. As per 3 dB SNR increase in the high SNR regime leads to a per-user sum-rate increase of $\min(1, 1/\beta)$ bits/s/Hz [12, 13], we have $G_{c\infty} = G_p/3\min(1, 1/\beta)$.

4.1. Optimization for $\gamma = 4$

As a uniform closed-form expression for $\mathcal{G}(a,b)$ in (19) is hard to obtain for all γ, we deal with a typical path loss exponent of 4 in this section. Then, (19) becomes:

$$\begin{aligned}\mathcal{G}^{(4)}(a,b) &= \exp\left(\frac{1}{2}\lambda^2\sigma_s^2\right)\frac{1}{\pi}\int_0^{\pi}\frac{1}{\left(a^2+b^2-2ab\cos\theta\right)^2}\,d\theta \\ &= \exp\left(\frac{1}{2}\lambda^2\sigma_s^2\right)\frac{a^2+b^2}{\left|a^2-b^2\right|^3}.\end{aligned} \tag{29}$$

To get $\mathcal{P}^{(4)}(a)$, we further express the pdf of user polar radius (7) as

$$f_B(b) = \frac{2b}{A}, \quad b \in [0, \max(0, a-R_0)] \cup [\min(R, a+R_0), R], \tag{30}$$

where $A = (\max(0, a-R_0))^2 + \max(0, R^2 - (a+R_0)^2)$. Substituting (29) and (30) into (24), we have

$$\begin{aligned}\mathcal{P}^{(4)}(a) = \frac{1}{A}\big(&f(0) - f(\max(0, a-R_0)) \\ &+ f(R) - f(\min(R, a+R_0))\big),\end{aligned} \tag{31}$$

where

$$\begin{aligned}f(t) = \exp\left(-\frac{1}{2}\lambda^2\sigma_s^2\right)\Big(&\frac{t^6}{3} - 2a^2t^4 + 7a^4t^2 \\ &- 8a^6\ln\left(a^2+t^2\right)\Big).\end{aligned} \tag{32}$$

Since in a practical system $R_0 \ll R$, we can rewrite $\mathcal{P}^{(4)}(a)$ in (31) to the following piecewise form:

$$\begin{aligned}&\mathcal{P}^{(4)}(a) \\ &= \begin{cases} \dfrac{f(R) - f(a+R_0)}{R^2 - (a+R_0)^2}, & 0 \le a < R_0, \\ \dfrac{f(0) - f(a-R_0) + f(R) - f(a+R_0)}{(a-R_0)^2 + R^2 - (a+R_0)^2}, & R_0 \le a \le R - R_0, \\ \dfrac{f(0) - f(a-R_0)}{(a-R_0)^2}, & R - R_0 < a \le R. \end{cases}\end{aligned} \tag{33}$$

A closed-form rate-power relationship is then obtained by substituting (33) into (26).

For a path loss exponent of 4, the optimal radius for antenna deployment is the one that minimizes (33). Therefore, $a_{\text{opt}}^{(4)}$ satisfies $(\partial\mathcal{P}^{(4)}(a)/\partial a)|_{a_{\text{opt}}^{(4)}} = 0$ and $(\partial^2\mathcal{P}^{(4)}(a)/\partial^2 a)|_{a_{\text{opt}}^{(4)}} > 0$, or it is one of the endpoints of the intervals in (33). Given R and R_0, we can find $a_{\text{opt}}^{(4)}$ numerically. Consider $R = 2000$ m and $R_0 = 20$ m according to the COST231-Walfish-Ikegami model [14], we find that $a_{\text{opt}}^{(4)} = 1352$ m and $\mathcal{P}^{(4)}(a_{\text{opt}}^{(4)}) = 5.988 \cdot 10^{11} \cdot \exp(-(1/2)\lambda^2\sigma_s^2)$. Substituting $\mathcal{P}^{(4)}(a_{\text{opt}}^{(4)})$ into (26), the rate-power relationship of OCL-DAS becomes

$$C_{\text{OCL-DAS}}^{(4)} = \mathcal{C}\left(\beta, \frac{E \cdot \exp\left((1/2)\lambda^2\sigma_s^2\right)}{5.988 \cdot 10^{11}\sigma_n^2}\right). \tag{34}$$

CAS is a special case of CL-DAS with $a = 0$. According to (33), we have $\mathcal{P}^{(4)}(0) = 5.334 \cdot 10^{12} \cdot \exp(-(1/2)\lambda^2\sigma_s^2)$ and

$$C_{\text{CAS}}^{(4)} = \mathcal{C}\left(\beta, \frac{E \cdot \exp\left((1/2)\lambda^2\sigma_s^2\right)}{5.334 \cdot 10^{12}\sigma_n^2}\right). \tag{35}$$

Comparing (34) and (35), we find that OCL-DAS offers a power gain of $G_p^{(4)} = 10\log(53.34/5.988) = 9.498$ dB or a per-user sum-rate gain in high SNR regime of $G_{c\infty}^{(4)} = 3.166 \cdot \min(1, 1/\beta)$ bits/s/Hz over CAS. We note that shadowing only impacts $\mathcal{P}(a)$ by a scalar multiplication of $\exp(-(1/2)\lambda^2\sigma_s^2)$ and thus does not impact the value of the optimal radius.

4.2. Optimization for an arbitrary γ

For most practical systems, the path loss exponent is not an integer, which makes the closed-form expression for (24) hard to obtain. To find the optimal radius for an arbitrary γ, we present a numerical optimization method. This method

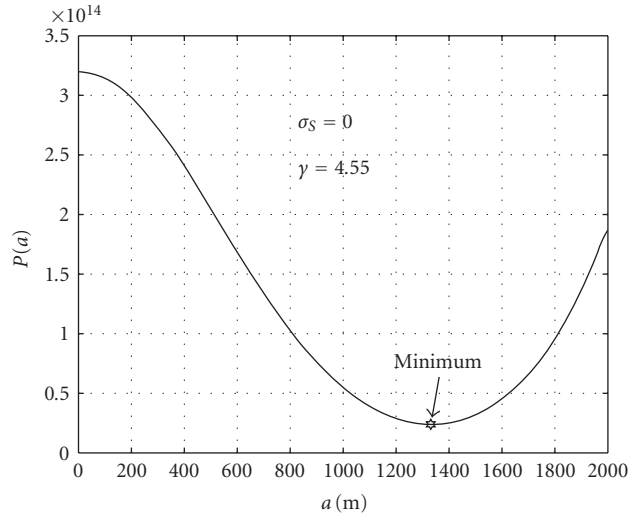

Figure 2: Numerical result of $\mathcal{P}(a)$ for $\gamma = 4.55$ and $\sigma_s = 0$.

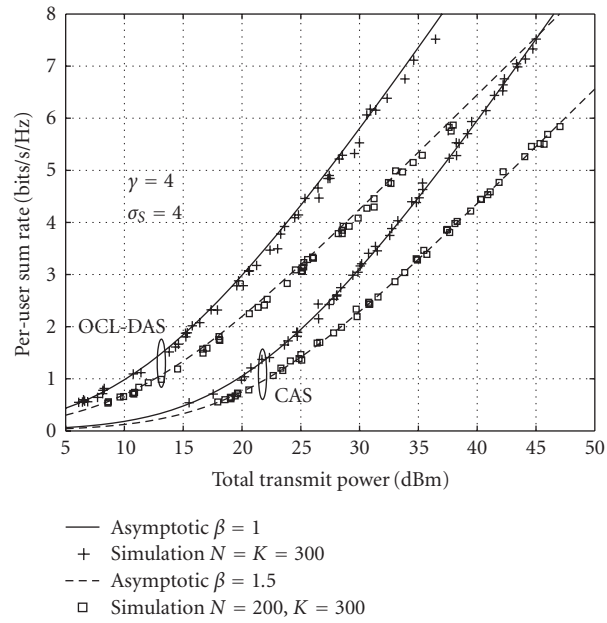

Figure 3: Simulation results for a large-scale system with $\gamma = 4$.

is widely applicable but with high computational complexity. We use COST231-Walfish-Ikegami model [14] to find a practical γ, since it covers antenna height of less than 10 m, which is common for DAS. We take a scenario with the following parameters as an example: mobile station height l.5 m, antenna height 10 m, building height 20 m, and street width 20 m [8]. Under these conditions, γ becomes 4.55.

$R = 2000$ m and $R_0 = 20$ m are considered here. Then, a may vary from 0 to 2000 m. We set the increasing step to 1 m, so a takes value in $\{0, 1, \ldots, 2000\}$ m. To calculate (24) for each a, we set the increasing step of b to 1 m. For each (a, b) pair, we calculate $\mathcal{G}(a, b)$ in (19) numerically. With these $\mathcal{G}(a, b)$s, we calculate (24) for each a, and thus we get $\mathcal{P}^{(4.55)}(a)$ as plotted in Figure 2 for $\sigma_s = 0$. For other σ_s, only a scalar multiplication of $\exp(-(1/2)\lambda^2\sigma_s^2)$ to the presented result is needed. The numerical result shows the optimal a that minimizes $\mathcal{P}^{(4.55)}(a)$ is $a_{\text{opt}}^{(4.55)} = 1331$ m and $\mathcal{P}^{(4.55)}(a_{\text{opt}}^{(4.55)}) = 2.394 \cdot 10^{13} \cdot \exp(-(1/2)\lambda^2\sigma_s^2)$, so the rate-power relationship of OCL-DAS becomes

$$C_{\text{OCL-DAS}}^{(4.55)} = \mathcal{C}\left(\beta, \frac{E \cdot \exp\left((1/2)\lambda^2\sigma_s^2\right)}{2.394 \cdot 10^{13}\sigma_n^2}\right). \tag{36}$$

As $\mathcal{P}^{(4.55)}(0) = 3.195 \cdot 10^{14} \cdot \exp(-(1/2)\lambda^2\sigma_s^2)$, the rate-power relationship of CAS is

$$C_{\text{CAS}}^{(4.55)} = \mathcal{C}\left(\beta, \frac{E \cdot \exp\left((1/2)\lambda^2\sigma_s^2\right)}{3.195 \cdot 10^{14}\sigma_n^2}\right). \tag{37}$$

Comparing (36) and (37), we find that OCL-DAS offers a power gain of $G_p^{(4.55)} = 10\log(31.95/2.394) = 11.25$ dB or a per-user sum-rate gain in high SNR regime of $G_{c\infty}^{(4.55)} = 3.751 \cdot \min(1, 1/\beta)$ bits/s/Hz over CAS.

5. SIMULATION RESULTS

5.1. Simulation for a large-scale system

In this section, we verify the validity of our analysis via large-scale system simulation, where there are a large number of antennas and users. Noise power σ_n^2 is -107 dBm given 5 MHz bandwidth and -174 dBm/Hz thermal noise as in the universal mobile telecommunications system (UMTS). The shadowing standard deviation is set to 4 according to field measurement for microcell environment [15].

Figure 3 presents simulation results for $\gamma = 4$, which has been studied in Section 4.1. According to the analysis, antennas are mutually independent and uniformly distributed on the circle of $r = 1352$ m for OCL-DAS, while they are centralized at the center for CAS. For each set of parameters in this figure, 50 independent realizations are carried out. In each realization, the required receiving power P_R is generated according to uniform distribution in $[-110, -80]$ dBm; antenna positions, user locations, shadowing and $\mathbf{H}_w$ are generated according to aforementioned distributions; then the per-user sum rate and the total transmit power are calculated and plotted according to (12) and (13), respectively. The rate-power relationships for OCL-DAS (34) and CAS (35) are also plotted for comparison. We can draw from the plots that the simulated results converge to the rate-power relationship for both OCL-DAS and CAS. OCL-DAS outperforms CAS by nearly 10 dB in power efficiency for both $\beta = 1$ and $\beta = 1.5$, which agrees well with our analysis. As for the sum rate, OCL-DAS offers nearly 3 bits/s/Hz per user for $\beta = 1$ and 2 bits/s/Hz per user for $\beta = 1.5$ in the high transmit power regime, which validates the analytical results.

Figure 4 presents simulation results for $\gamma = 4.55$, which has been studied in Section 4.2. According to the analysis, an-

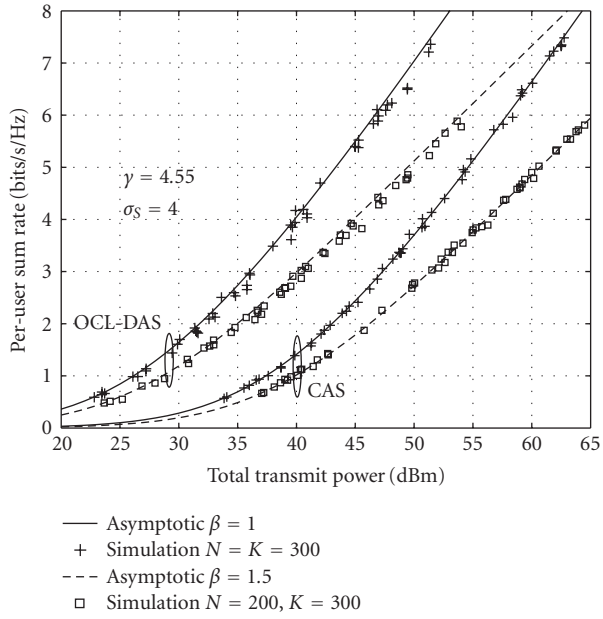

Figure 4: Simulation results for a large-scale system with $\gamma = 4.55$.

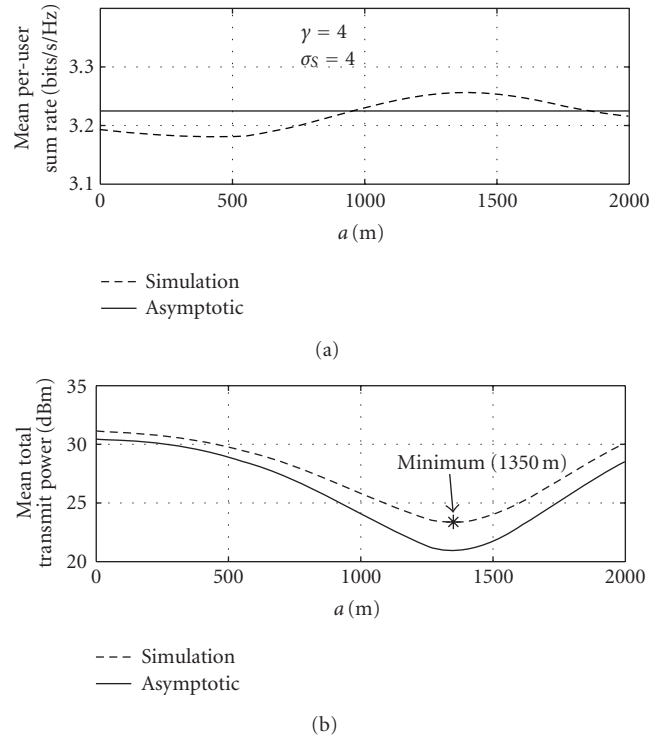

Figure 5: Simulation results for a practical system scale ($N = K = 8$).

tennas are mutually independent and uniformly distributed on the circle of $r = 1331$ m for OCL-DAS. P_R is also generated according to uniform distribution in $[-110, -80]$ dBm. The analytical relationships (36) and (37) for $\gamma = 4.55$ are also plotted. As the plots demonstrate, the simulated results converge to the asymptotic expression for both OCL-DAS and CAS, and OCL-DAS outperforms CAS by more than 11 dB in power efficiency for both $\beta = 1$ and $\beta = 1.5$, which agrees well with our analysis. In the high transmit power regime, the per-user sum-rate gain is nearly 3.5 bits/s/Hz per user for $\beta = 1$ and 2.5 bits/s/Hz per user for $\beta = 1.5$, which also verifies the validity of our analysis.

5.2. Simulation for a practical system scale

From a practical point of view, we investigate the applicability of the analysis and the asymptotically optimal circle radius to a practical system scale, for example, eight antennas and eight users. Though we consider a random deployment of antennas and a random distribution of users in the asymptotic analysis, it is inefficient to adopt this scheme in a system with a small number of antennas, since the totally random scheme may result in, with a considerable probability, unbalanced load among antennas. For a small-scale system, we consider a more efficient scheme with regularly deployed antennas. We assume the coordinates of the nth antenna are $(a, ((n-1)\pi/4))$, $n = 1, 2, \ldots, 8$. These antennas divide the circular area into eight congruent sectors with the polar angle of the nth sector satisfying $\theta_n \in [((n-1)\pi/4) - \pi/8, ((n-1)\pi/4) + \pi/8)$, $n = 1, 2, \ldots, 8$. We also assume that the eight simultaneously-accessing users are located in the eight distinct sectors, which can be achieved via user selection.

In this simulation, only a path loss exponent of 4 is considered. Since we need to investigate the applicability of the asymptotically optimal radius, performances for all possible a are simulated with the P_R set to a medium value -95 dBm. Considering the tradeoff between computational complexity and accuracy, we set the increasing step of a to 10 m, so a takes value in $\{0, 10, \ldots, 2000\}$ m. Performance of the asymptotically optimal radius 1352 m is also simulated. For a small-scale system, the instantaneous per-user sum-rate is subject to a large variation and thus less valuable. So we evaluate the mean per-user sum rate and the mean total transmit power averaged over 10^5 realizations. Since the rate-power relationship for a small-scale system may differ from the asymptotic relationship, we examine the mean per-user sum rate and the mean total transmit power separately with results displayed in Figure 5. We can draw from this figure that the mean per-user sum rate differs little (less than 2%) from the asymptotic analysis. Though the difference between the mean total transmit power and the asymptotic result is noticeable, the two curves coincide well in shape. More importantly, difference between the simulated optimal radius 1350 m and the asymptotically optimal radius 1352 m is small and OCL-DAS saves nearly 8 dB total transmit power compared with CAS. Hence, the deployment optimization method is applicable in practice and OCL-DAS provides a significant gain even when the system scale is small.

5.3. Simulation for a multi-cell environment

As shown in the previous sections, OCL-DAS in an isolated area offers significant power gain and capacity gain over CAS. However, in a multicell environment, as antennas are dis-

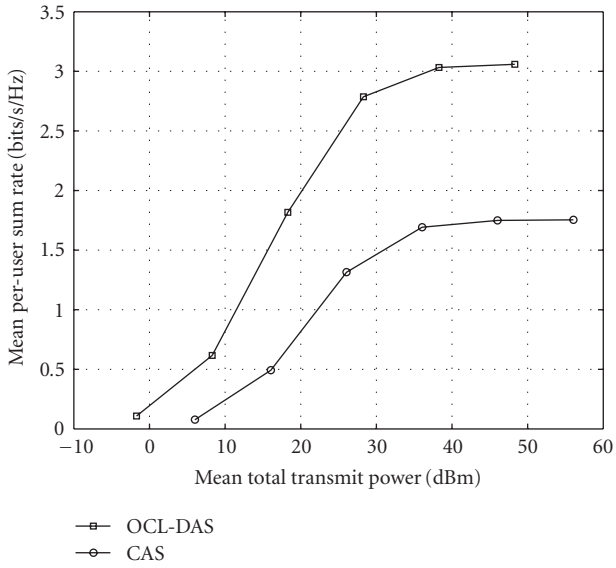

Figure 6: Performance of OCL-DAS in a multicell environment ($N = K = 8$).

tributed far from the cell center, they may suffer from more inter-cell interference. To estimate the impact of the inter-cell interference, we present simulation results of OCL-DAS in a multi-cell environment. Since a multi-cell system with sufficient frequency reuse can be regarded as consisting of several isolated areas, which have been analyzed in the previous parts, we consider the worst case with universal frequency reuse in the following simulation. We assume that the interferences only come from the neighboring cells, and a one-tier cell structure is considered. Since we are interested in the performance of a practical OCL-DAS, small-scale system with the same configuration as in Section 5.2 is considered for each cell. For fair comparison between OCL-DAS and CAS, we assume each cell processes its receiving signals independently and simply treats signals from other cells as interference.

In the multi-cell simulation, the required receiving power P_R varies from -120 dBm to -70 dBm. Figure 6 displays simulation results for both OCL-DAS and CAS. From the plot, we find that when the transmit power is relatively small, the system is noise-limited and acts like an isolated cell. In this situation, OCL-DAS offers a power gain of nearly 10 dB over CAS. As transmit power increases, the system becomes interference-limited, and increasing transmit power does not lead to a further capacity increase. In this regime, OCL-DAS reaches it capacity limit of 3.1 bits/s/Hz per user, while the capacity limit is 1.8 bits/s/Hz per user for CAS. Therefore, OCL-DAS offers a capacity gain of 1.3 bit/s/Hz per user over CAS. Though it is not as large as in an isolated cell environment, the capacity improvement is significant.

6. CONCLUSIONS

We have proved that for a CL-DAS, the per-user sum rate and the total power consumption both converge as user number and antenna number go to infinity with a constant ratio. Then, the relationship between the asymptotic per-user sum rate and the asymptotic total transmit power is established. Based on this relationship, the optimal radius for antenna deployment has been found. The optimized CL-DAS has been shown to offer power gains of 9.498 dB and 11.25 dB over CAS for path loss exponents of 4 and 4.55, respectively. We believe that these gains are not the best we can achieve by scattering antennas and with some better antenna topologies it is possible to get even higher system performances.

APPENDIX

PROOF OF PROPOSITION 2

Consider the power-controlled equivalent channel $\mathbf{H_E} = \mathbf{L}\sqrt{K}\mathbf{P}^{1/2} \circ \mathbf{H}_w$, where $\mathbf{H}_w$ is a matrix with independent, zero mean, unit variance, circularly symmetric complex Gaussian entries. To apply Proposition 1, we investigate the asymptotic edf of each row and each column of the equivalent power gain matrix $\mathbf{G_E}$ which consists of $\mathbf{G_E}_{n,k} = Kp_k\mathbf{L}^2_{n,k} = Kp_k\mathbf{G}_{n,k} = (KP_R\mathbf{G}_{n,k}/\sum_{n=1}^{N}\mathbf{G}_{n,k})$.

We first check edf of each column of $\mathbf{G_E}$. For an arbitrary user with index k and polar radius b, its corresponding power gain vector $\mathbf{G_E}_{:,k}$ consists of $(KP_R\mathbf{G}_{1,k}/\sum_{n=1}^{N}\mathbf{G}_{n,k})$, $(KP_R\mathbf{G}_{2,k}/\sum_{n=1}^{N}\mathbf{G}_{n,k})$, …, $(KP_R\mathbf{G}_{N,k}/\sum_{n=1}^{N}\mathbf{G}_{n,k})$. Since $\mathbf{G}_{1,k}, \mathbf{G}_{2,k}, \ldots, \mathbf{G}_{N,k}$ are i.i.d. random variables with cdf (17), by the strong law of large numbers, edf of $(\mathbf{G_E}_{:,k})^T$ converges almost surely, as $N, K \to \infty, K/N \to \beta$, to the cdf of a random variable $(G_E \mid B = b) = (\beta P_R \cdot (G \mid B = b)/\mathcal{E}[G \mid B = b])$, where $(G \mid B = b)$ is a random variable with cdf (17). The expectation of $(G_E \mid B = b)$ is

$$\mathcal{E}[G_E \mid B = b] = \beta P_R, \tag{A.1}$$

which is independent of user index k and user polar radius b. Since $R_0 \le D < 2R$, $\mathcal{G}(a,b)$ in (18) satisfies

$$\exp\left(\frac{1}{2}\lambda^2\sigma_s^2\right)\cdot(2R)^{-\gamma} < \mathcal{G}(a,b) \le \exp\left(\frac{1}{2}\lambda^2\sigma_s^2\right)\cdot R_0^{-\gamma}, \tag{A.2}$$

then for all q, the qth moment of $(G_E \mid B = b)$ is bounded:

$$\begin{aligned}
&\mathcal{E}[G_E^q \mid B = b] \\
&\quad = \left(\frac{\beta P_R}{\mathcal{G}(a,b)}\right)^q \cdot \mathcal{E}[D^{-\gamma q} \mid B = b] \cdot \mathcal{E}[S^q] \\
&\quad < \left(\frac{\beta P_R}{\exp\left((1/2)\lambda^2\sigma_s^2\right)\cdot(2R)^{-\gamma}}\right)^q \cdot R_0^{-\gamma q} \cdot \exp\left(\frac{1}{2}\lambda^2\sigma_s^2 q^2\right) \\
&\quad = (\beta P_R)^q \left(\frac{2R}{R_0}\right)^{\gamma q} \exp\left\{\frac{1}{2}\lambda^2\sigma_s^2 q(q-1)\right\}.
\end{aligned} \tag{A.3}$$

In the same way, the edf of each row of $\mathbf{G_E}$ converges almost surely to the cdf of a random variable G_E with $F_{G_E}(g) = \int_{b\in\mathcal{B}} F_{G_E|B}(g \mid b) f_B(b)\mathrm{d}b$. The expectation of G_E is

$$\mathcal{E}[G_E] = \mathcal{E}[\mathcal{E}[G_E \mid B]] = \beta P_R, \tag{A.4}$$

and for all q, the qth moment of G_E is bounded:

$$\begin{aligned}\mathcal{E}\left[G_E^q\right] &= \mathcal{E}\left[\mathcal{E}\left[G_E^q \mid B\right]\right] \\ &< (\beta P_R)^q \left(\frac{2R}{R_0}\right)^{\gamma q} \exp\left\{\frac{1}{2}\lambda^2\sigma_s^2 q(q-1)\right\}.\end{aligned} \tag{A.5}$$

We have shown that $\mathbf{H_E}$ satisfies Proposition 1, except that the expectation of the asymptotic edf of each column and each row of $\mathbf{G_E}$ is βP_R. With some necessary normalization, we conclude that as $N, K \to \infty$ with $K/N \to \beta$, (12) converges almost surely to

$$\mathcal{C}\left(\beta, \frac{\beta P_R}{\sigma_n^2}\right). \tag{A.6}$$

ACKNOWLEDGEMENTS

This work was supported by China's 863 Beyond 3G Project Future Technologies for Universal Radio Environment (FuTURE) under Grant 2003AA12331002 and National Natural Science Foundation of China under Grant 90204001.

REFERENCES

[1] W. Rhee and J. M. Cioffi, "On the capacity of multiuser wireless channels with multiple antennas," *IEEE Transactions on Information Theory*, vol. 49, no. 10, pp. 2580–2595, 2003.

[2] A. A. M. Saleh, A. J. Rustako Jr., and R. S. Roman, "Distributed antennas for indoor radio communications," *IEEE Transactions on Communications*, vol. 35, no. 12, pp. 1245–1251, 1987.

[3] H. Zhuang, L. Dai, L. Xiao, and Y. Yao, "Spectral efficiency of distributed antenna system with random antenna layout," *Electronics Letters*, vol. 39, no. 6, pp. 495–496, 2003.

[4] M. V. Clark, T. M. Willis III, L. J. Greenstein, A. J. Rustako Jr., V. Erceg, and R. S. Roman, "Distributed versus centralized antenna arrays in broadband wireless networks," in *Proceedings of the 53rd IEEE Vehicular Technology Conference (VTS '01)*, vol. 1, pp. 33–37, Rhodes, Greece, May 2001.

[5] G. J. Foschini, H. C. Huang, K. Karakayali, R. A. Valenzuela, and S. Venkatesan, "The value of coherent base station coordination," in *Proceedings of the 39th Annual Conference on Information Sciences and Systems (CISS '05)*, The Johns Hopkins University, Baltimore, Md, USA, March 2005.

[6] O. Somekh, B. M. Zaidel, and S. Shamai, "Sum-rate characterization of multi-cell processing," in *Proceedings of the Canadian Workshop to Information Theory (CWIT '05)*, Montreal, Quebec, Canada, June 2005.

[7] M. N. Bacha, J. S. Evans, and S. V. Hanly, "On the capacity of cellular networks with MIMO links," in *Proceedings of IEEE International Conference on Communications (ICC '06)*, vol. 3, pp. 1337–1342, Istanbul, Turkey, June 2006.

[8] J. H. Lee, J. H. Roh, and C. E. Kang, "Reverse link capacity analysis of DS-CDMA system with distributed antennas using selection diversity," *Electronics Letters*, vol. 36, no. 23, pp. 1962–1963, 2000.

[9] M.-S. Alouini and A. J. Goldsmith, "Area spectral efficiency of cellular mobile radio systems," *IEEE Transactions on Vehicular Technology*, vol. 48, no. 4, pp. 1047–1066, 1999.

[10] E. Telatar, "Capacity of multi-antenna Gaussian channels," *European Transactions on Telecommunications*, vol. 10, no. 6, pp. 585–595, 1999.

[11] A. M. Tulino, L. Li, and S. Verdú, "Spectral efficiency of multicarrier CDMA," *IEEE Transactions on Information Theory*, vol. 51, no. 2, pp. 479–505, 2005.

[12] A. M. Tulino, A. Lozano, and S. Verdú, "Impact of antenna correlation on the capacity of multiantenna channels," *IEEE Transactions on Information Theory*, vol. 51, no. 7, pp. 2491–2509, 2005.

[13] A. M. Tulino, S. Verdú, and A. Lozano, "Capacity of antenna arrays with space, polarization and pattern diversity," in *Proceedings of IEEE Information Theory Workshop (ITW '03)*, pp. 324–327, Paris, France, March-April 2003.

[14] G. L. Stüber, *Principles of Mobile Communication*, Kluwer Academic Publishers, Boston, Mass, USA, 2nd edition, 2001.

[15] A. J. Goldsmith and L. J. Greenstein, "Measurement-based model for predicting coverage areas of urban microcells," *IEEE Journal on Selected Areas in Communications*, vol. 11, no. 7, pp. 1013–1023, 1993.